Large eddy simulation of flow past a twisted cylinder

Jae Hwan Jung
Department of Naval Architecture and Ocean Engineering
Pusan National University
Pusan, KOREA
vof@pusan.ac.kr

Hyun Sik Yoon
Global Core Research Center for Ships and Offshore Plants
Pusan National University
Pusan, KOREA
lesmodel@pusan.ac.kr

Abstract— **The wavy cylinder has a sinusoidal variation in cross sectional area along the spanwise direction and the twisted cylinder has been newly designed by rotating the elliptic cross section along the spanwise direction, so that the cylinder surface has a twisted spiral pattern. A twisted cylinder is investigated to observe the effect of twisted spiral pattern of the flow fields. It guarantees the accuracy of the present numerical methods that the excellent comparisons with previous studies for the cases of a smooth circular cylinder. The effect of surface torsion which is newly designed in here has been predicted and assessed in terms of the mean drag and root-mean-square (RMS) value of fluctuating lift at the subcritical Reynolds number of 3000. Subsequently, the mechanisms of enhancing the aerodynamic performance and passive control of vortex-induced vibrations are also investigated by careful analysis with the flow structures. The iso-surface of swirling strength has been imposed to identify the vortical structures in the turbulent wake.**

Keywords—twisted cylinder; drag; lift

I. INTRODUCTION (*Heading 1*)

Flow around cylindrical structure has been widely investigated for over a large range of Reynolds numbers because of a lot of their fundamental significance in flow physics. Among the physical phenomena of the flow past cylindrical structure, the generation and evolution of vorticies in the wake region are important in practical application of engineering [1-3]. It produces a drag and fluctuating lift forces and vortex-induced vibration that affect aerodynamic performance such as the mean drag and fluctuating lift forces. Thus, a number of researchers for over a century effort to understand and to control the dynamics of the wake vortices with the aim of reducing the mean drag and fluctuating lift forces [4-9].

One of some forms of three-dimensional (3D) geometric disturbances for passive controlling is a waviness of a cylinder. It has the sinusoidal variation in the cross sectional area along the spanwise direction to consider its effect on the flow characteristics such as the wake vortices. Ahmed and Bays-Muchmore [4] investigated experimentally the transverse flow over a wavy cylinder. They demonstrated that the sectional drag coefficient at the node was greater than that at the saddle and that the significant spanwise pressure gradients resulted in 3D flow separation. Lee and Nguyen [5] investigated experimentally the drag force, mean velocity and turbulence intensity profiles of the wake behind a wavy cylinder in the range of Re = 5000–20,000. They found that wavy cylinders reduced drag coefficient compared with the smooth cylinder and the wake structure varied periodically along the spanwise direction. Lam et al. [6] found that the mean drag coefficients and fluctuating lift coefficients of wavy cylinders were lower than those of the smooth cylinder in the range of Re = 20,000–50,000. A drag reduction of up to 20% can be achieved. Lam et al. [7] investigated the flow characteristics experimentally in the range of Re = 3000–9000. They concluded that the average vortex formation length to over half a wavelength of the wavy cylinder was longer than that of the smooth cylinder, resulting in drag reduction and suppression of the vortex-induced vibration. Lam and Lin [8] found that the mean drag and fluctuating lift of wavy cylinder are less than those of a corresponding circular cylinder in some range of wavelength representing waviness of cylinder surface by using the large eddy simulation.

Another approach to handle the dynamics of the wake vortices is a twisted cylinder in passive control. The twisted cylinder has been newly designed by rotating the elliptic cross section along the spanwise direction, so that the cylinder surface has a twisted spiral pattern. The twisted cylinder has not been thoroughly investigated, whereas the flow fields behind wavy cylinders have been extensively examined. Therefore, the purpose of the present study is to investigate the flow characteristics of the twisted cylinder. In order to simulate the flow past the twisted cylinder, large eddy simulation (LES) have been employed at subcritical Reynolds number of 3000, where subcritical Reynolds means that the boundary layer remains laminar on the cylinder surface and the wake is completely turbulent after flow separation. Finally, the flow characteristics of twisted cylinder have been compared with those of the circular and the wavy cylinder at same Re to observe the effect of the twisted spiral pattern applied on the circular cylinder.

II. NUMERICAL DETAILS

A. *Large eddy simulation*

We describe briefly the mathematical formulation for the dynamic model, which will be employed here for the

simulation of the flow past twisted cylinder. For the incompressible, constant property flow considered here, the basic governing equation for the large eddy evolution are the grid filtered Navier-Stokes and continuity equations.

$$\frac{\partial \overline{u}_j}{\partial x_j} = 0 \tag{1}$$

$$\frac{\partial \overline{u}_i}{\partial t} + \frac{\partial \overline{u}_i \overline{u}_j}{\partial x_j} = -\frac{1}{\rho}\frac{\partial \overline{p}}{\partial x_i} + \nu \frac{\partial^2 \overline{u}_i}{\partial x_j \partial x_j} - \frac{\partial \tau_{ij}}{\partial x_j} \tag{2}$$

where overbar denotes the large (or resolved) scale flow obtained from grid-filtering. In (1) and (2), x_i are Cartesian coordinates, u_i are the corresponding velocity components, t is the time, p is the pressure, and Re is the Reynolds number. The effect of the subgrid scale motion on the dynamics of the resolved velocity is accounted for by the subgrid scale stress tensor

$$\tau_{ij} = \overline{u_i u_j} - \overline{u}_i \overline{u}_j \tag{3}$$

which is modeled by the dynamic smagorinsky model [10] in order to obtain a closure for (1) and (2). Further details of the mathematical formulation for the dynamic model refer to [10] and [11].

B. Definition of the Body Geometries

The several cylindrical structures such as the cylinder, wavy and the twisted cylinder are shown in Fig. 1. The circular cylinder is the well known as the typical simple geometry in fluid mechanics, as shown in Fig. 1(a). The geometry of the wavy cylinder is described by $D_z = D_m + 2a\cos(2\pi z/\lambda)$. Here, D_z is the normalized local diameter, D_m is the normalized mean diameter, a is the normalized amplitude of the surface curve, λ is the normalized wavelength, and z is the spanwise location. The normalized mean diameter of the wavy cylinder is defined with $D_m = D_{max} + D_{min}/2$. The axial locations of the maximum diameter (D_{max}) are here after termed 'node', while the axial locations of the minimum

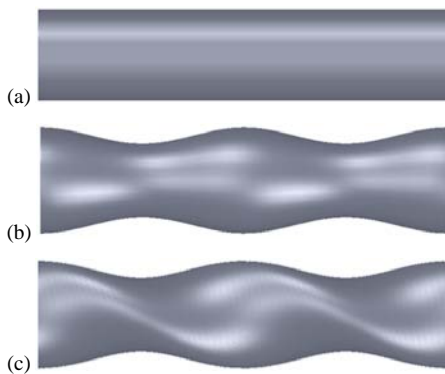diameter (D_{min}) are denoted as 'saddle'. The wavy cylinder is as shown in Fig. 1(b). The twisted cylinder has been newly designed by rotating the elliptic cross section along the spanwise direction, so that the cylinder surface has a twisted spiral pattern as shown in Fig. 1(c). The normalized mean diameter of twisted cylinder is defined with $(A+B)/2$, where A is the length of the major axis, also referred as major diameter is the same as D_{max}, and B is the length of the minor axis, also referred as minor diameter is the same as D_{min} in elliptic cross section. Note that the mean diameter of the wavy and the twisted cylinder has the value of same diameter of the circular cylinder.

C. Computational Domain and Boundary condtions

The computational domain placed a cylinder of mean diameter D_m at the center of a circular and extends over $32D_m$ in the streamwise and normal directions. The spanwise extent of the domain was chosen to be $4.55D_m$, which corresponds to the size used by Lam and Lin [8], as shown in Fig. 2. The inflow and outflow boundary conditions are applied on outer surface. The uniform velocity profile is imposed at the inlet boundary, whereas convective boundary condition $\partial u_i / \partial t + c \partial u_i / \partial x = 0$ is imposed on the outflow region, where c is the space-averaged streamwise inlet velocity. On the surface of the body, no-slip and no-penetration conditions are adopted. Neumann type boundary condition is used for pressure. A periodic boundary condition is adopted in a spanwise direction considering an infinitely long cylindrical
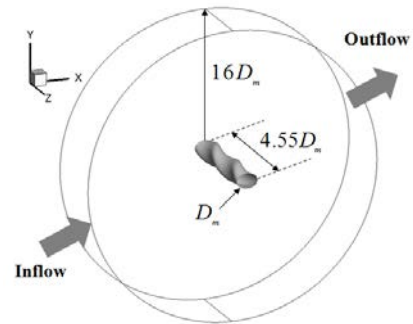

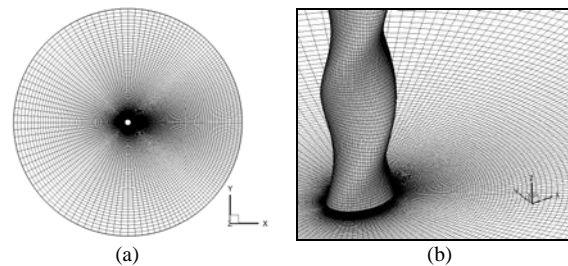Fig. 2 Schematic of the computational domain and boundary condition.

(a)   (b)

Fig. 3 Grid distributions around twisted cylinder (a) entire domain, (b) region about cylinder and near wake.

(a)

(b)

(c)

Fig. 1 Geometry of the different type of (a) circular, (b) wavy and (c) twisted cylinder.

structure.

Fig. 3 shows the grid over the entire computational domain and close to the twisted cylinder surface. In order to capture accurately the separating shear layers on the surface of the twisted cylinder, the grids are distributed non-uniformly near its surface. The distance from the cylinder surface to the nearest grid points are fixed at $y^+ = 1$.

D. Grid Dependence Test

Three different grid systems (coarse, medium and fine grids) were considered to test the grid dependence of the solutions for the circular cylinder. The results of present computations summarized in table 1 are found to be in fairly good agreement with the experimental data (Norberg, [12]; Norberg, [13]) and slightly smaller than those of 3D simulation results by Lam et al. [8]. Grid independence tests are satisfied considering the variation of the values such as mean drag, fluctuating lift, Strouhal number with the different grid systems. For the twisted cylinder, the dependence of the solutions on the grid systems summarized in table 2 was also not strong. Consequently, the medium grid system was selected for all cases.

TABLE 1 GRID DEPENDENCE TEST FOR A CIRCULAR CYLINDER

Case	$N_r \times N_\theta \times N_z$	$\overline{C_D}$	$C_{L,RMS}$	St
Noberg [12]	Experimental	0.98-1.03	N/A	0.210-0.213
Noberg [13]	Summarized	N/A	0.05, 0.07	0.210
Lam and Lin [8]	$16,000 \times 80$	1.09	0.177	0.210
Coarse	$127 \times 127 \times 80$	1.00	0.123	0.213
Medium	$146 \times 146 \times 80$	0.99	0.115	0.212
Fine	$163 \times 163 \times 80$	1.00	0.122	0.210

TABLE 2 GRID DEPENDENCE TEST FOR A TWISTED CYLINDER

Case	$N_r \times N_\theta \times N_z$	$\overline{C_D}$	$C_{L,RMS}$	St
Coarse	$127 \times 127 \times 80$	0.88	0.0052	0.191
Medium	$146 \times 146 \times 80$	0.86	0.0050	0.190
Fine	$163 \times 163 \times 80$	0.85	0.0045	0.182

E. Validations

Three different grid systems (coarse, medium and fine grids) were considered to test the grid dependence of the solutions for the circular cylinder. The results of present computations summarized in table 1 are found to be in fairly good agreement with the experimental data (Norberg, [12]; Norberg, [13]) and slightly smaller than those of 3D simulation results by Lam et al. [8]. Grid independence tests are satisfied
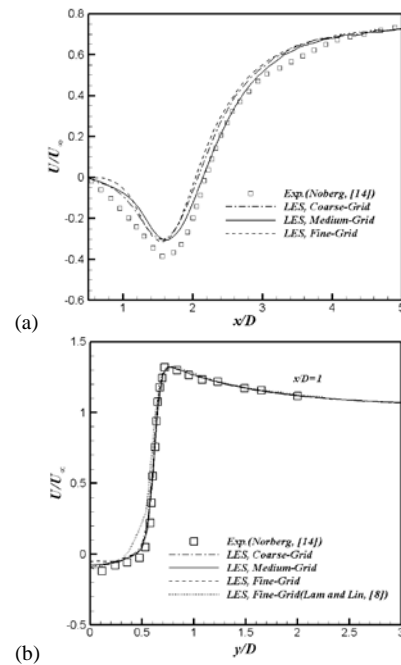

(a)

(b)

Fig. 4 Mean streamwise velocity U / U_∞ along the (a) wake centerline, (b) wake vertical line.

considering the variation of the values such as mean drag, fluctuating lift, Strouhal number with the different grid systems. For the twisted cylinder, the dependence of the solutions on the grid systems summarized in table 2 was also not strong. Consequently, the medium grid system was selected for all cases.

In the near wake of a circular cylinder at Reynolds number of 3000, mean streamwise velocities along the wake center line and vertical line were compared with experimental data by Noberg [14], respectively, as shown in Fig. 4. The present results of U / U_∞ along the wake center line show a little difference with the experimental data by Noberg [14] in $0 \le x / D \le 2$ regardless of the different grid systems, as shown in Fig. 4 (a). However, only very little discrepancy can be observed between the present results and experimental result in $x / D > 2$. The present results of U / U_∞ along the wake vertical line for the different grid systems agree well with the experimental data by Noberg [14] whereas an a little difference of the values of U / U_∞ can be observed from the LES results of Lam et al. [8] and experimental data by Noberg [14], as shown in Fig. 4 (b). As a results, our LES results of U / U_∞ are in good qualitative and quantitative agreement with experimental data by Noberg [14] regardless of the different grid systems.

III. RESULTS AND DISCUSSION

A. Forces and Strouhal Numbers of the DifferentType Cylinder

In order to enhance the aerodynamic performance, it is important to reduce the mean drag and fluctuating lift related to

vortex-induced vibration. Namely, the dynamic force coefficients are good criterions to assess aerodynamic performance. Table 3 shows that the values of the mean drag, fluctuating lift coefficient and Strouhal number are summarized for the different type cylinders. All the values such as mean drag and fluctuating lift coefficients of the twisted cylinder are the smallest of the three different cylinders. The drag coefficient reduction up to 14% is obtained and the fluctuating lift coefficient is also considerably suppressed compared with the circular and the wavy cylinder. From the results, it seems that the spiral pattern applied on the circular cylinder may significantly control the vortex structures and reduce the drag and the fluctuating lift coefficient. The Strouhal numbers of the wavy cylinder is roughly the same as that of the circular cylinder, but that for twisted cylinder is smaller than that of the circular and the wavy cylinder. That is, the geometry of the wavy surface may have no effect on the frequency of vortex shedding for the cylinders while the twisted spiral pattern applied on the cylinder affect the frequency of vortex shedding.

TABLE 3 COMPARISON OF THE FORCE COEFFICIENTS AND STROUHAL NUMBER FOR THE DIFFERENT CYLINDER

Type	$\overline{C_D}$	$C_{L,RMS}$	St
Circular	0.99	0.1150	0.211
Wavy	0.91	0.0244	0.213
Twisted	0.86	0.0045	0.182

B. Instantaneous vortical structures

Fig. 5 shows the instantaneous vortical structures at Reynolds number of 3000 for the different cylinders. The iso-surface of swirling strength has been imposed to identify the vortical structures in the turbulent wake. Further details of this vortex identification method were given in the previous works which was conducted by Zhou et al. (1999). The fully turbulent wake behind the circular cylinders is represented by small eddies, but small scale eddies are hardly observed at further downstream position due to a coarse grid resolution that was produced by grid clustering on the cylinder surface. However, its formation clearly shows the primary Karman vortex street as shown in Fig. 5 (a).

The separating shear layer of the circular cylinder interact with a pairs of vortices from the upper and lower part of the rear side in the near wake region, then the vortex shedding occurs to the downstream.

For the twisted cylinder, the shear layer is more elongated to the downstream and the swirling vortex shed far from the body than that of the circular and the wavy cylinder as observed in Fig. 5 (a)-(c). As a result, vortex shedding process is delayed and the wake width shrinks to the downstream direction causing significant reduction of fluctuating lift when the twisted spiral pattern is applied on the cylinder.

As shown in Fig. 5 (a), a lot of the small scale eddies in the right behind the circular cylinder are observed, but the
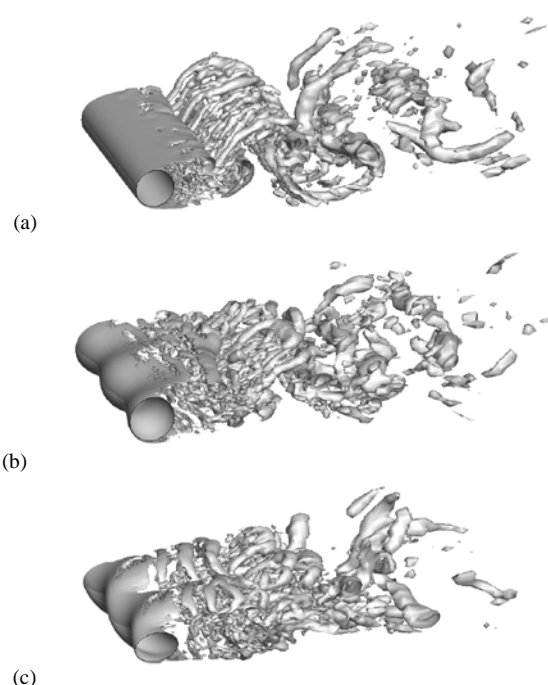

(a)

(b)

(c)

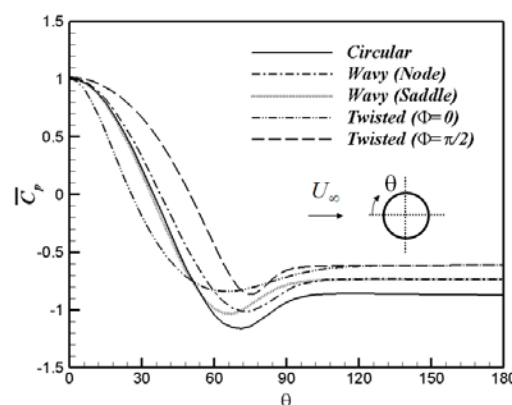Fig. 5 Instantaneous vortical structures of the (a) Circular, (b) wavy and (c) twisted cylinder.

Fig. 6 Distribution of time-averaged pressure coefficient on the cylinder surface

positions of the small scale eddies are farther away from the back of the twisted cylinder than that of the circular and the wavy cylinder as shown in Fig. 5 (a)-(c). It may be concluded that the vortex strength in the near wake of the twisted cylinder may be weaker than that of the circular and the wavy cylinder and the base pressure of the twisted cylinder can be increased, causing considerable reduction of the drag.

C. Distribution of Time-averaged Pressure Coefficient on the Cylinder Surface

Fig. 6 shows the profile of time-averaged pressure coefficient on the cylinder surface as a function of circumferential angle of θ. In the line legend, $\Phi = 0$ denotes the torsion phase angle when the major axis is parallel to the free stream direction, $\Phi = \pi / 2$ denotes the major axis is

perpendicular to the free stream direction. With increasing θ from the stagnation point, the mean pressure coefficient of the circular cylinder have the intermediate values between those of the wavy cylinder with node and saddle, however the distinct differences are observed after about $\theta = 51$. At about $\theta = 71$, the mean pressure coefficients of the circular cylinder reaches the maximum value of negative suction pressure. After about $\theta = 112$, all the values of mean pressure coefficient are converged corresponding to the each base pressure for the different cylinders and the maximum negative suction pressure coefficients of twisted cylinder with $\Phi = 0$ and $\Phi = \pi / 2$ are the smallest in all cases as shown in Fig. 6. By the comparison pressure distribution on the cylinder surface, it has been shown that the pressure drag of the twisted cylinder is the lowest of the three different cylinders.

D. Turbulent kinetic energy distribution

Fig. 7 shows the contour plots of the turbulent kinetic energy (TKE) in the x–y planes of the wake behind the twisted cylinder with $\Phi = 0$ and $\Phi = \pi / 2$ compared with that of the circular and wavy cylinder at $Re = 3000$. For the circular cylinder, the region of prominent TKE distribution with the maximum TKE values is in the right behind the circular cylinder which has the largest TKE values of the three different cylinders. In case of the wavy cylinder, the maximum TKE values and the high TKE values regime in the nodal plane are larger that of the saddle plane. It is similar to the LES results obtained by Lam et al. [8]. Unlike case of the wavy cylinder, only very little discrepancy can be observed between the TKE values at $\Phi = 0$ and $\Phi = \pi / 2$ for the twisted cylinder and the maximum TKE values and the high TKE values of the twisted cylinder are the smallest of the three different cylinders. Furthermore, the positions of maximum TKE are farther away from the back of the twisted cylinder than that of the circular and wavy cylinder as shown Fig. 7(a)-(e). It may be concluded that the twisted cylinder may considerably reduce the TKE in the near wake and can get more TKE reduction than the wavy cylinder.

IV. Conclusion

The flow around a twisted cylinder newly designed by rotating the elliptic cross section along the spanwise direction at a subcritical Reynolds number (Re) of 3000 is investigated using large eddy simulation. The instantaneous vortical structures of the twisted cylinder are compared with those of the circular and the wavy cylinder at the same Re. The shear layer of the twisted cylinder covering the recirculation region is more elongated than those of the circular and the wavy cylinder, and then vortex shedding of the twisted cylinder is considerably suppressed. Consequently, the mean drag coefficient and the fluctuating lift of the twisted cylinder are less than those of the circular and the wavy cylinder. It is also confirmed by the results of the distribution of the mean pressure on the cylinder surface.

For turbulent kinetic energy (TKE) distribution, it can be observed that the twisted cylinder may considerably reduce the TKE in the near wake and can get more TKE reduction than
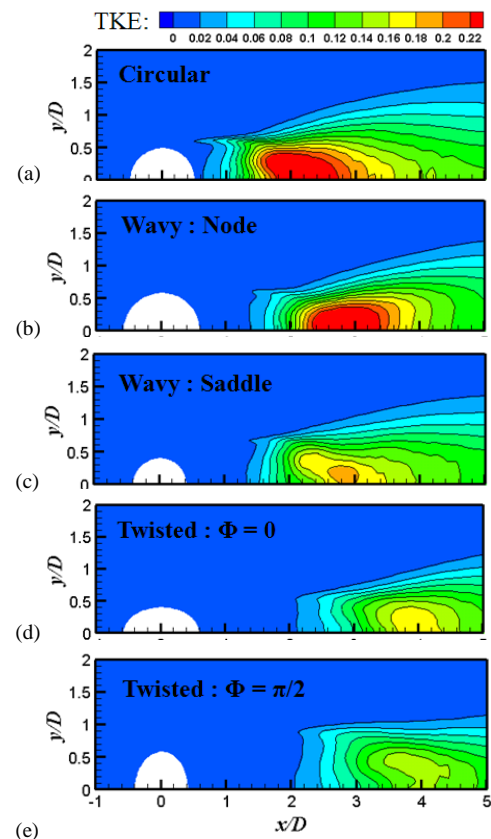

Fig. 7 Turbulent kinetic energy distributions in x-y planes of the wake behind the (a) circular, (b-c) wavy and (d-e) twisted cylinder.

the wavy cylinder. The present study simply focus on the flow structures, the distribution of the mean pressure on the cylinder surface and turbulent kinetic energy distribution instead of providing whole physical explanation. However, we can clearly observe the effect on the spiral pattern causing significantly reduction of mean drag and fluctuating lift.

References

[1] C.H.K. Williamson, "Oblique and parallel modes of vortex shedding in the wake of a circular cylinder at low Reynolds numbers," J. Fluid Mech., vol. 206, pp.579−628. 1989.

[2] C.H.K. Williamson, "Vortex dynamics in the cylinder wake," Ann. Rev. Fluid Mech., vol. 28, pp.477−539, 1996.

[3] M. F. Unal and D. Rockwell, "On vortex formation from a cylinder. Part 1. The initial instability," J. Fluid Mech., vol.190, pp.491-512, 1977.

[4] A. Ahmed and B. Bays-Muchmore, "Transverse flow over a wavy cylinder," Phys. Fluids A, vol. 9, no. 4, pp.1959−1967, 1992.

[5] S. Lee, A.T. Nguyen, "Experimental investigation on wake behind a wavy cylinder having sinusoidal cross-sectional area variation," Fluid Dyn. Res., vol.39, pp.292−304, 2007.

[6] K. Lam, F. H. Wang, J. Y. Li, R. M. C. So, "Experimental investigation of the mean and fluctuating forces of wavy (varicose) cylinders in a cross-flow," J. Fluids Struct., vol.19, pp.321-334, 2004.

[7] K. Lam, F. H. Wang R. M. C. So, "Three-dimensional nature of vortices in the near wake of a wavy cylinder," J. Fluids Struct.,vol.19, pp. 815−833, 2004.

[8] K. Lam and Y. F. Lin, "Large eddy simulation of flow around wavy cylinders at a subcritical Reynolds number," Int. J. Heat Fluid Flow vol. 29, pp.1071-1088, 2008.

[9] R. Mittal and S. Balachandar, "Direct numerical simulation of flow past elliptic cylinders," J. Comput. Phys.,vol.124, pp.351−367, 1994.

[10] M. Germano, U. Piomelli, P. Moin and W.H. Cabot, "A Dynamic subgrid-scale eddy viscosity model," Phys. Fluids A, vol.3, pp.1760, 1991.

[11] H. S. Yoon, S. Balachandar, M. Y. Ha, "Large eddy simulation of flow in an unbaffled stirred tank for different Reynolds numbers," Phys. Fluids, vol. 21, pp.1-16, 2009.

[12] C. Norberg, Effects of Reynolds number and a low-intensity freestream turbulence on the flow around a circular cylinder, Department of Applied Thermodynamics and Fluid Mechanics, Chalmers University of Technology, 1987.

[13] C. Norberg, "Fluctuating lift on a circular cylinder: review and new measurements," Journal of Fluids and Structures, vol.17, pp.57–96, 2003.

[14] C. Norberg, LDV-measurements in the near wake of a circular cylinder. In: Proc. the ASME Fluids Eng. Div. Summer Meeting, Washington, FED-Vol. 245, 1998, FEDSM98-5202.